Stochastic Mixing of Bound Thermal Scattering Data in MONK

Simon Richards*

ANSWERS Software Service, Wood, Kings Point House, Queen Mother Square, Poundbury, Dorchester, DT1 3BW, United Kingdom.

Abstract

The Monte Carlo neutronics code MONK® uses run-time Doppler broadening to achieve highly accurate temperature interpolation. However the tabulated $S(\alpha, \beta)$ data which are used to compute the secondary energies and angles in bound thermal scattering interactions do not lend themselves to interpolation, and it is therefore recommended to use the closest tabulated temperatures. In some cases this can lead to significant step changes in reactivity at the mid-point between two tabulated temperatures. The implementation and testing of a stochastic mixing approach to avoid this approximation are described. Results from two test cases are presented: the first decouples the effect of moderator density and demonstrates that the stochastic mixing removes the step changes in reactivity seen when using the nearest temperature approach; and the second is a more physically-realistic model at reactor operating conditions, which demonstrates that the nearest temperature approach does not introduce significant errors in thermal LEU systems if the moderator density is varied with temperature in a physically-realistic way.

Keywords: Monte Carlo, MONK, bound thermal scattering, temperature interpolation

1. Introduction

1.1. MONK

MONK® is an advanced Monte Carlo neutronics code for the solution of criticality safety and reactor physics problems. It has a proven track record of application to the whole of the nuclear fuel cycle and is well established as the *de facto* standard criticality code in the UK criticality community. Furthermore it is increasingly being used for reactor physics applications.

The current version of MONK is MONK10B, which was released in 2017 after an extensive programme of enhancements over the previous versions [1, 2]. MONK continues to be actively developed and new features and enhancements, including those described in the current work, will be incorporated into the next release, MONK11A [3].

*Corresponding author

Email address: simon.richards@woodplc.com (Simon Richards)

MONK's advanced geometry modelling and detailed, continuous-energy collision treatment provides realistic 3D models for an accurate simulation of neutronic behavior. MONK calculates the k_{eff} for the system modelled using a staged (or iterative) calculation, with each stage consisting of a fixed number of neutron *superhistories* [4]. A neutron superhistory is the set of tracks followed by a neutron and its fission progeny from birth to absorption or leakage, through a fixed number of fission generations. The maximum generation number is typically 10, although this can be changed under user control, and setting this number to 1 reduces superhistory powering to conventional history powering as used in other Monte Carlo criticality codes.

MONK can perform calculations using a range of collision processing techniques and data libraries including: the BINGO point energy neutron collision processor and BINGO format continuous energy nuclear data libraries; the DICE point energy neutron collision processor and hyperfine group data (13,193 energy groups); and broad group collision processing using WIMS [5] subgroup data in the standard WIMS 172 group libraries.

The use of the BINGO collision processor and data gives the highest accuracy with the best representation of the physics, including run-time Doppler broadening [6] such that any material can be represented at any temperature (above the base temperature of the available BINGO libraries) with the minimum of user effort (all the user needs to do is specify the temperature of the material). The ability to treat continuous temperature variation is of particular importance when modelling thermal feedback in coupled neutronics and thermal hydraulics calculations.

1.2. Bound thermal scattering

For neutrons with energies below a few eV, the thermal motions of scattering nuclides profoundly affect the outcome of collisions. There are three important processes that occur here:

- inelastic thermal scatter – a colliding neutron may either gain or lose energy from the motions of a bound target nucleus and some of the kinetic energy may be transferred to excited molecular quantum levels, e.g. rotation, vibration;
- incoherent elastic scatter – the wave-like behaviour of the neutron combined with the random nature of some scattering media gives rise to incoherent elastic scatter where the neutron is scattered without change of energy. The angular distribution of the scattered neutrons is forward peaked and continuous; and
- coherent elastic scatter – if the nuclei of the scattering medium are arranged in a well-defined array (i.e. a crystalline material) then coherent elastic scatter may occur. Scattering takes place into well-defined directions that are a function of the wavelength of the incident neutron and the lattice parameters. This type of scattering is supported by the BINGO collision processor in MONK, but not by the older DICE collision processor.

For inelastic thermal scattering the cross-sections are given through the use of an $S(\alpha, \beta)$ function that is obtained from the analysis of the collisions using quantum mechanics. The data describing the $S(\alpha, \beta)$ function for a set of pre-determined temperatures are available in the form of evaluated nuclear data files. This type of scatter is especially important for bound hydrogen, and MONK currently uses these data for

hydrogen in water, hydrogen in polythene and hydrogen in zirconium hydride. The ENDF/B-VII libraries also include these data for zirconium in zirconium hydride and silicon and oxygen in silicon dioxide (ENDF/B-VII.1 only), and MONK is able to utilize these data.

MONK also treats incoherent elastic scatter for hydrogen in polythene, hydrogen in zirconium hydride and, for ENDF/B-VII, zirconium in zirconium hydride. This type of scattering is negligible for hydrogen in water. Coherent elastic scatter data are present for graphite, beryllium metal and beryllium oxide, and are utilized by the BINGO collision processor in MONK.

Thermal scattering in all other nuclides is treated by applying a monatomic free-gas model. Even for bound nuclei, the monatomic gas model is applied when the incident energy is well in excess of the energy levels for internal oscillations. The run-time broadening method cannot be used for bound thermal scattering data and so additional data are stored on the library to allow for temperature interpolation. These additional data are stored for the temperatures at which $S(\alpha, \beta)$ data are given in the evaluated files. The $S(\alpha, \beta)$ temperatures for each library are given in Table 1. Currently, an interpolation method is applied to the thermal scattering cross-sections but not to the secondary (emitted) data which are taken from the nearest $S(\alpha, \beta)$ temperature. In certain cases, this can result in a significant change in reactivity for a small change in temperature, particularly where the temperature is near the mid-point between one $S(\alpha, \beta)$ temperature and the next. This article describes the implementation and testing of a commonly-used method to overcome this limitation in an idiomatically Monte Carlo way to smoothly interpolate the bound thermal scattering secondary data in temperature.

Nuclide	**JEFF-3.x and CENDL-3.1**	**ENDF/B-VII.x**
H in H_2O	293.6, 323.6, 373.6, 423.6, 473.6, 523.6, 573.6, 623.6, 647.2, 800.0, 1000.0	293.6, 350.0, 400.0, 450.0, 500.0, 550.0, 600.0, 650.0, 800.0
H in CH_2	293.6, 350.0	296.0 350.0
H in ZrH	293.6, 400.0, 500.0, 600.0, 700.0, 800.0, 1000.0, 1200.0	296.0, 400.0, 500.0 600.0, 700.0, 800.0 1000.0, 1200.0
D in D_2O	293.6, 323.6, 373.6, 423.6, 473.6, 523.6, 573.6, 643.9	293.6, 350.0, 400.0, 450.0, 500.0, 550.0, 600.0, 650.0
C in graphite	293.6, 400.0, 500.0, 600.0, 700.0, 800.0, 1000.0, 1200.0, 1600.0, 2000.0, 3000.0	296.0 400.0, 500.0, 600.0, 700.0, 800.0, 1000.0, 1200.0, 1600.0, 2000.0
Be and O in BeO	296.6, 400.0, 500.0, 600.0, 700.0, 800.0, 1000.0, 1200.0	296.6, 400.0, 500.0, 600.0, 700.0, 800.0, 1000.0, 1200.0
Be in Be metal	296.0, 400.0, 500.0, 600.0, 700.0, 800.0, 1000.0, 1200.0	296.0, 400.0, 500.0, 600.0, 700.0, 800.0, 1000.0, 1200.0
Z in ZrH	Not available	296.0 400.0, 500.0, 600.0, 700.0, 800.0, 1000.0, 1200.0
Si and O in SiO_2	Not available	293.6, 350.0, 400.0, 500.0, 800.0, 1000.0, 1200.0

Table 1: Temperatures (K) at which $S(\alpha, \beta)$ data are tabulated in the BINGO nuclear data libraries [7].

2. Methods

In the BINGO collision processor in MONK the temperature of any material may be set to any temperature T_{broad} above the base temperature of the BINGO library (this is 293.6 K for currently released BINGO libraries but will be extended to lower temperatures for future libraries). If T_{broad} is within 0.5 K of a BINGO library temperature then the Doppler broadened nuclear cross-sections are obtained directly from the library file,

otherwise run-time Doppler broadening is employed to determine the Doppler broadened cross-section at temperature T_{broad}.

The $S(\alpha, \beta)$ data needed to calculate secondary parameters for bound thermal scattering are stored in the BINGO library at a small number of fixed temperatures, and there is no straightforward way of interpolating these data analytically. The ENDF-6 Formats Manual [8] states that "Experience has shown that temperature interpolation of $S(\alpha, \beta)$ data is unreliable. It is recommended that cross sections be computed for the given moderator temperatures only. Data for other temperatures should be obtained by interpolation between the cross sections." This recommendation is followed in the BINGO collision processor and the inelastic scattering cross section is interpolated between the temperatures at which the $S(\alpha, \beta)$ data are given. However, this simple interpolation is not applicable to the calculation of secondary energy and angle, and the BINGO collision processor therefore uses the $S(\alpha, \beta)$ data at the closest tabulated temperature.

For $T_1 \leq T_{\text{broad}} \leq T_2$, where T_1 and T_2 are the two adjacent tabulated temperatures bounding T_{broad}, the following condition is tested:

$$|T_1 - T_{\text{broad}}| \leq |T_2 - T_{\text{broad}}| \tag{1}$$

If this condition is true then the $S(\alpha, \beta)$ data tabulated at T_1 are used, otherwise the data at T_2 are used. In the stochastic mixing method we replace this deterministic selection of the $S(\alpha, \beta)$ data with a sampling method which randomly selects the data tabulated at T_1 and T_2 with probabilities based on where T_{broad} lies in the range T_1 to T_2.

The probability p_1 of selecting the data at the lower temperature T_1 is given by:

$$p_1 = \frac{(T_2 - T_{\text{broad}})}{(T_2 - T_1)} \tag{2}$$

At each collision the following condition is tested:

$$\xi < p_1 \tag{3}$$

where ξ is a pseudo-random number in the range 0 to 1, taken from a uniform distribution. If this condition is satisfied then the $S(\alpha, \beta)$ data at T_1 are used, otherwise the data tabulated at T_2 are used. As a new pseudo-random number is sampled at each collision the effect is to randomly choose the T_1 data with probability p_1 and the T_2 data with probability $p_2 = 1 - p_1$.

The results of the sampling algorithm for all possible temperature values are shown in Table 2. Special cases exist if T_{broad} is less than the lowest tabulated temperature or greater than the highest tabulated temperature. In these cases the value of p_1 will be greater than 1 or less than 0 respectively. Although these are strictly not valid probabilities the correct result is obtained when evaluating the conditional expression.

It is noted that the stochastic mixing method has been commonly employed in Monte Carlo neutronics codes for several decades. However, perhaps because it falls into the category of "obvious" computational techniques, it appears not to have been well documented in the literature.

The method described in this section has been implemented as an option in the BINGO collision processor in the current development version of MONK11A alongside the existing nearest temperature approach, such that the two methods may be compared.

Temperature	p_1	Result
$T_{\text{broad}} < T_1$	$p_1 > 1$	T_1 is always used (only occurs if T_1 is the lowest tabulated value)
$T_{\text{broad}} = T_1$	$p_1 = 1$	T_1 is always used
$T_1 < T_{\text{broad}} < T_2$	$0 < p_1 < 1$	T_1 is used with probability p_1 T_2 is used with probability $1 - p_1$
$T_{\text{broad}} = T_2$	$p_1 = 0$	T_2 is always used
$T_{\text{broad}} > T_2$	$p_1 < 0$	T_2 is always used (only occurs if T_2 is the highest tabulated value)

Table 2: Results of the stochastic sampling algorithm.

3. Example calculations

3.1. Single pincell

3.1.1. Model description

A single pincell integration test has been used to demonstrate the effect of the stochastic mixing method. This test case consists of a single 3.82 wt% enriched UO_2 unclad fuel rod of radius 0.48 cm, in the centre of a water-filled box with x and y dimensions of 1.2 cm. Reflecting boundary conditions are applied on all faces to represent an infinite array of fuel rods with a pitch of 1.2 cm. The hydrogen is modelled as ^{1}H bound in water and the oxygen is modelled as ^{16}O.

The fuel temperature in this model is fixed at 500.0 K and the water temperature is varied between 293.6 K (the base temperature of a standard BINGO library) and 1100.0 K (which is greater than the maximum $S(\alpha, \beta)$ tabulated temperature for water in the JEFF-3.2 BINGO library used. Calculations are performed at each of the eleven tabulated temperatures (see Table 1) and additionally at points 0.1 K above and below the mid-points between each library temperature in order to demonstrate the step change in k_∞ at the mid-points. A final point at 1100.0 K is used to demonstrate the behaviour at temperatures above the maximum $S(\alpha, \beta)$ tabulated temperature. A corresponding point below the minimum temperature of 293.6 K is not permitted since it is below the base temperature of the BINGO library.

It is important to note that the water density is kept fixed at 0.99 g/cc for all temperatures in this integration test to allow the effect of the bound thermal scattering model to be decoupled from any effects of changing moderator density. While this is clearly non-physical it is not unusual for criticality safety analysts to model the moderator at the maximum expected or maximum theoretical density in order to maximize the reactivity, thereby ensuring that the criticality safety criterion is conservatively satisfied.

All MONK calculations were run with a target standard deviation of 0.0002 with the JEFF-3.2 BINGO library, using a development version of MONK11A [3]. The calculations were run in parallel using the OpenMPI version of MONK running on 16 cores of a Linux HPC.

3.1.2. Results

The results from the pincell test case are plotted in Figure 1. This shows the results of using the current nearest temperature treatment together with the results obtained

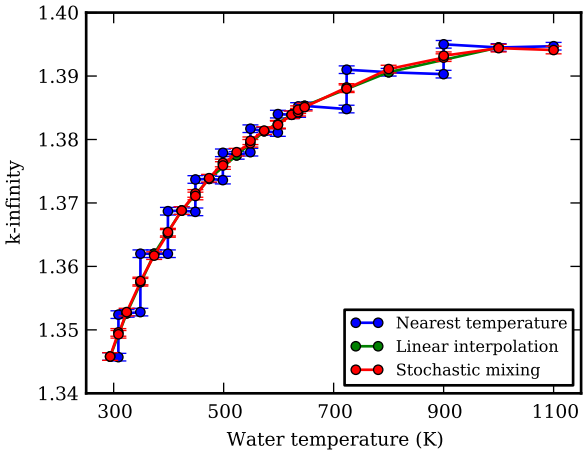

Figure 1: Results of the pincell integration test, comparing interpolation methods (error bars indicate ±3 standard deviations).Note that the linear interpolation curve is almost exactly over-plotted by the stochastic mixing curve.

using the stochastic mixing methodology described in Section 2. In addition to these two sets of results Figure 1 also shows the results obtained by linearly interpolating between results obtained at tabulated $S(\alpha, \beta)$ temperatures only, i.e. points between tabulated temperatures are obtained by linearly interpolating between the results calculated at the two bounding tabulated temperatures.

The results obtained using the nearest temperature approach show the expected step changes at the mid-points between tabulated temperatures where the collision processor switches from the data at the lower bounding temperature to the data at the upper bounding temperature. These step changes are non-physical and are an artefact of using the nearest temperature data without interpolation.

The results obtained using the stochastic mixing method completely eliminate the step changes seen in the results based on nearest temperature values and are statistically equivalent to the linear interpolation approach without requiring any post-processing. The two methods agree, to within the stochastic uncertainty, at the tabulated temperatures, and the stochastic mixing method correctly interpolates at intermediate temperatures, giving confidence that the method behaves as intended.

Table 3 shows the differences between the results obtained using the nearest temperature method and the stochastic mixing method at temperatures 0.1 K either side of the mid-points between adjacent tabulated temperatures. These results indicate that, for this model, using the nearest temperature approach can underestimate the multiplication by up to 470 pcm for temperatures just below the mid-point, and overestimate the multiplication by up to 430 pcm for temperatures just above the mid-point. The combined standard deviation from the pairs of calculations from which these differences are obtained is about 28 pcm.

Temperature (K)	k_∞		Δk (pcm)
	Nearest	Interpolated	
308.5	1.3457 ± 0.0002	1.3496 ± 0.0002	-390 ± 28
308.7	1.3524 ± 0.0002	1.3493 ± 0.0002	+310 ± 28
348.5	1.3528 ± 0.0002	1.3575 ± 0.0002	-470 ± 28
348.7	1.3620 ± 0.0002	1.3577 ± 0.0002	+430 ± 28
398.5	1.3620 ± 0.0002	1.3652 ± 0.0002	-320 ± 28
398.7	1.3687 ± 0.0002	1.3654 ± 0.0002	+330 ± 28
448.5	1.3686 ± 0.0002	1.3715 ± 0.0002	-290 ± 28
448.7	1.3737 ± 0.0002	1.3711 ± 0.0002	+260 ± 28
498.5	1.3736 ± 0.0002	1.3763 ± 0.0002	-270 ± 28
498.7	1.3779 ± 0.0002	1.3759 ± 0.0002	+200 ± 28
548.5	1.3780 ± 0.0002	1.3794 ± 0.0002	-140 ± 28
548.7	1.3817 ± 0.0002	1.3798 ± 0.0002	+190 ± 28
598.5	1.3811 ± 0.0002	1.3824 ± 0.0002	-130 ± 28
598.7	1.3840 ± 0.0002	1.3823 ± 0.0002	+170 ± 28
635.3	1.3841 ± 0.0002	1.3843 ± 0.0002	-20 ± 28
635.5	1.3852 ± 0.0002	1.3847 ± 0.0002	+50 ± 28
723.5	1.3848 ± 0.0002	1.3882 ± 0.0002	-340 ± 28
723.7	1.3910 ± 0.0002	1.3880 ± 0.0002	+300 ± 28
899.9	1.3903 ± 0.0002	1.3929 ± 0.0002	-260 ± 28
900.1	1.3950 ± 0.0002	1.3932 ± 0.0002	+180 ± 28

Table 3: Differences between the nearest temperature approach and the stochastic mixing approach at temperatures either side of the mid-points between adjacent tabulated temperatures. A negative difference indicates that the nearest temperature approach under-predicts relative to the interpolated method, while a positive difference indicates that the nearest temperature method over-predicts.

3.1.3. Run Time Performance

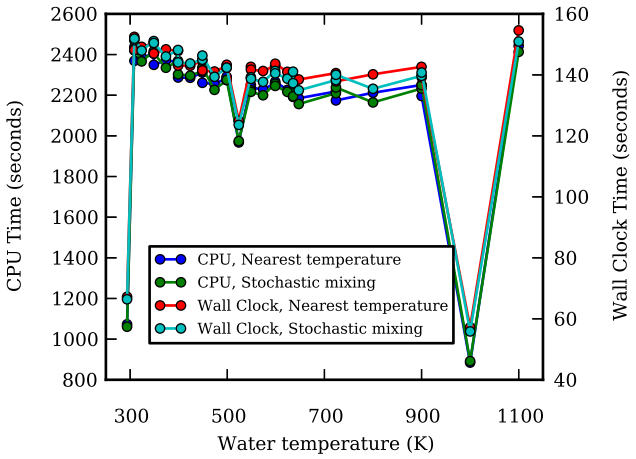

Figure 2: CPU Time and wall clock time for each calculation of the pincell test case running in parallel on 16 cores of a Linux HPC.

The single pincell test case described in Section 3.1.1 was run in parallel on 16 cores of a Linux HPC. The CPU times and elapsed ("wall clock") times for each calculation are shown in Figure 2. These results show that there is no significant, systematic difference in the run times between the two methods and that the stochastic mixing method does not add to the computational cost of the calculation.

It can be seen from these results that the 523.6 K calculations run in noticeably less time than most of the other calculations and that the 293.6 K and 1000.0 K runs are very significantly quicker, by more than a factor of two. This is to be expected because the BINGO library used for these calculations includes Doppler broadened cross-section data for both ^{16}O and ^{1}H in H_2O at 293.6 K and 1000.0 K, so the BINGO run-time Doppler broadening method is not invoked at all at these temperatures. At 523.6 K the library has Doppler broadened cross-section data for ^{1}H in H_2O, but not for ^{16}O, so the run-time Doppler broadening method is invoked for oxygen only in this calculation to Doppler broaden the cross-section from the 500 K library temperature to the 523.6 K moderator temperature.

3.2. PWR Minicore

3.2.1. Model description

In order to investigate the effect of stochastic mixing in a more physically-representative model under reactor-like conditions a 3x3 fuel assembly (FA) minicore model has been used [9]. The PWR fuel assemblies in this model are based on TMI-1, details of which are given in Table 4 and Table 5 [9]. Each assembly is a 15x15 array with 16 guide tubes, 1 instrumentation tube, and 208 Zircaloy clad fuel rods, four of which are gadolinia rods containing integral Gd burnable poisons. The mixture of the gadolinia rods is Gd_2O_3+UO_2 with density of 10.144 g/cc, enrichment of 4.12 wt% and Gd_2O_3 concentration of 2 wt%. The remaining fuel rods contain fresh UO_2 fuel (no burnup) with an enrichment of 4.85 wt% and density of 10.283 g/cc.

Parameter	**Value**
Unit cell pitch (mm)	14.427
Fuel pellet diameter (mm)	9.391
Fuel pellet material	UO_2
Fuel density (g/cc)	10.283
Fuel enrichment (wt%)	4.85
Cladding outside diameter (mm)	10.928
Cladding thickness (mm)	0.673
Cladding material	Zircaloy-4
Cladding density (g/cc)	6.55
Gap material	He (modelled as void)
Moderator material	H_2O

Table 4: Parameters of the TMI-1 fuel pincell used in the 3x3 PWR minicore model [9].

The 3x3 PWR minicore model comprises nine TMI-1 fuel assemblies as shown in Figure 3. The central assembly has the control rods fully inserted while the rest of the assemblies are modelled with control rods fully withdrawn.

Hot full power (HFP) conditions for the benchmark model are given in Table 6, but for the purposes of this investigation we replace the fixed moderator temperature and density with nominal, but physically reasonable, axial profiles as shown in Figure 5. The active length of the fuel rod is divided into ten equal slices having unique temperatures and densities, with two additional slices representing the upper and lower reflector regions, as shown in Figure 4. Event counts (unnormalized reaction rates) are tallied in the same axial regions. No attempt is made to modify the HFP critical boron concentration to account for the modified moderator temperatures and densities, so a small departure from critical conditions is to be expected. Since we are interested in the temperature dependence of the bound thermal scattering in the moderator, the fuel and clad temperatures retain their fixed HFP values so that the temperature dependence of the moderator is decoupled from other effects such as the Doppler broadening of the fuel resonances.

Parameter	Value
Fuel assembly dimensions	15 x 15
Number of fuel rods per FA	208
Number of guide tubes per FA	16
Number of instrumentation tubes per FA	1
Number of gadolinia rods per FA	4
Fuel rod pitch (mm)	14.427
Fuel rod outside diameter (mm)	10.922
Fuel pellet diameter (mm)	9.390
Cladding thickness (mm)	0.673
Guide tube outside diameter (mm)	13.462
Guide tube inside diameter (mm)	12.649
Instrumentation tube outside diameter (mm)	12.522
Instrumentation tube inside diameter (mm)	11.201
Fuel assembly pitch (mm)	218.110
Gap between fuel assemblies (mm)	1.702

Table 5: Parameters of the TMI-1 fuel assembly used in the 3x3 PWR minicore model [9].

Parameter	Value
Fuel temperature (K)	900.0
Clad temperature (K)	600.0
Moderator (coolant) temperature (K)	562.0
Moderator (coolant) density (g/cc)	0.7482

Table 6: Hot full power conditions for the TMI-1 PWR fuel assembly [9].

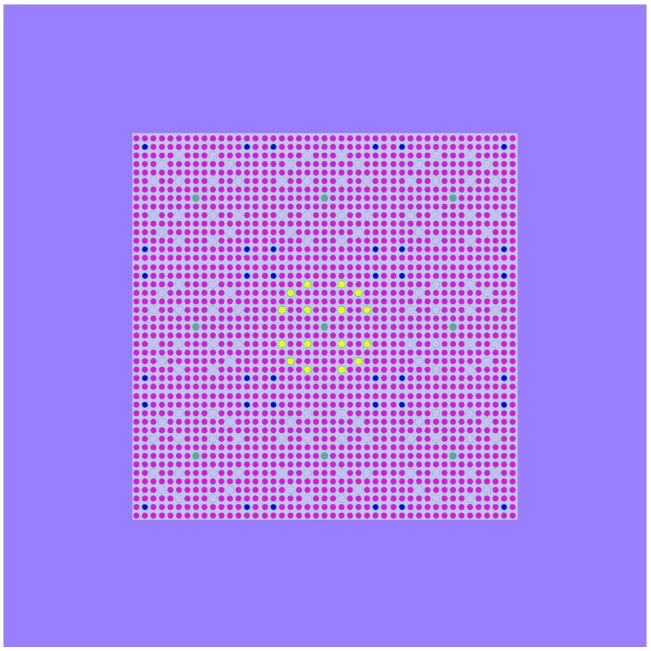

Figure 3: Radial slice of the 3x3 PWR minicore model, showing the nine fuel assemblies (the central one with control rods inserted) surrounded by the reflector (lilac). The control rods are shown in yellow and the Gd_2O_3+UO_2 integral burnable poison fuel rods are shown in dark blue.

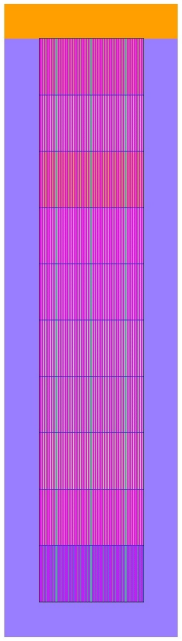

Figure 4: Axial slice of the 3x3 PWR minicore model, showing the active region divided into ten equal slices, the upper reflector material (orange) and the lower/radial reflector material (lilac).

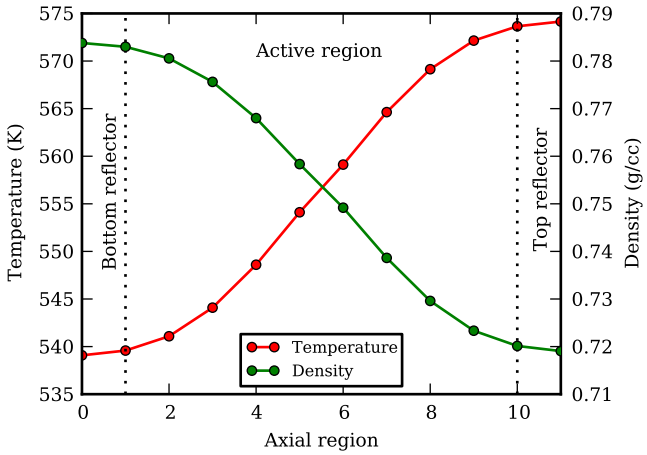

Figure 5: Axial temperature and density profiles used in the PWR minicore.

3.2.2. Results

Figure 6 compares the axial variation of the fission counts in the minicore model calculated using the nearest temperature approach and the stochastic mixing approach. This is the result of combining four independent calculations, each of which was run with 3 million post-settling (i.e. after the fission source distribution is converged) superhistories with a maximum of 100 generations per superhistory. This resulted in approximately 300 million neutron histories in each of the four calculations. The maximum stochastic error on the fission counts in any axial slice in each of the four calculations is less than 1%, so the maximum combined error for the four runs is less than 0.5%.

On the scale used in Figure 6 it is difficult to assess the differences between the two methods, so Figure 7 shows the difference between the two sets of calculations expressed as a percentage. Here it may be seen much more clearly that the nearest temperature method over-predicts the fission counts by up to about 2% in the lower axial regions, and under-predicts by up to about 3% in the upper axial regions, relative to the results obtained using the stochastic mixing method.

The combined results from the four independent calculations using the nearest temperature method gave a k_{eff} of 1.022573 ± 0.000027, while the result obtained using the stochastic mixing method gave 1.022591 ± 0.000027. These results agree to within the combined standard deviation, showing that the k_{eff} estimator in this case is not significantly altered by the stochastic mixing method.

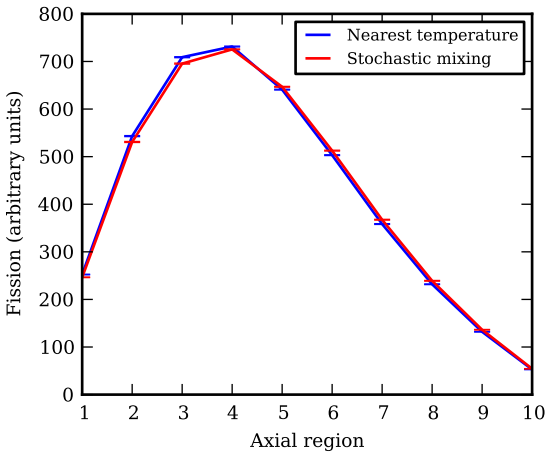

Figure 6: Axial variation of fission counts in the PWR minicore model, calculated using the nearest temperature approach and the stochastic mixing method.

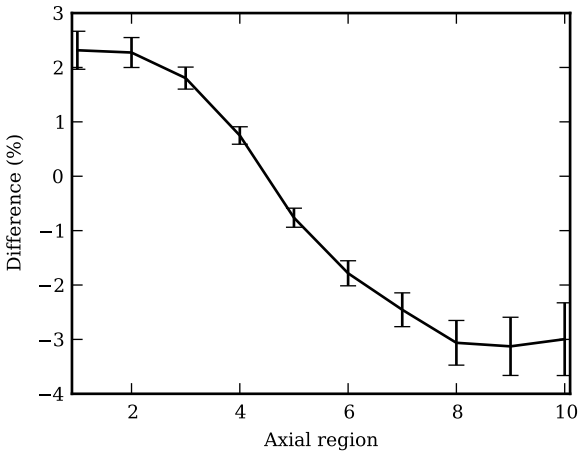

Figure 7: The relative difference [(nearest-interpolated)/interpolated] between the axial fission counts in the PWR minicore calculated using nearest temperatures and stochastic mixing. Negative values indicate that the nearest temperature approach under-predicts the fission counts relative to the interpolated approach, while positive values indicate that the nearest temperature approach over-predicts.

4. Conclusions

A stochastic mixing method has been implemented in the BINGO collision processor in a development version of MONK11 for interpolating the secondary data from bound thermal scattering reactions with respect to temperature. Instead of selecting the nearest tabulated temperature data the stochastic mixing method randomly selects either the upper or lower bounding temperature at each collision, with probabilities weighted according to how close the temperature is to the bounding temperatures.

Results presented for a single pincell model over a wide range of temperatures show the method to be working as expected with no run-time performance penalties. The stochastic mixing method eliminates the non-physical step changes in reactivity which can be observed near the mid-points between adjacent tabulated $S(\alpha, \beta)$ temperatures when using the nearest tabulated temperature approach. Although this model used the non-physical approach of fixing the moderator density over a wide range of temperatures, this is a conservative approach commonly used in criticality safety assessments, and therefore eliminating the approximation of using the nearest $S(\alpha, \beta)$ is a valuable improvement to MONK.

The results from a more physically-realistic model at reactor conditions showed no significant effect on the k_{eff} of the system, giving confidence that nearest temperature approximation does not introduce significant errors in k_{eff} for thermal, LEU systems when the moderator density is varied in a physically-realistic manner. However, small variations in the axial distribution of fission counts were observed which may be important in high fidelity burn-up or burn-up credit calculations, or when modelling thermal feedback in coupled neutronics and thermal hydraulics calculations.

Stochastic mixing is not an exact method, rather it is an approximation to using the correct temperature-dependent data. Nevertheless it has been shown to yield good results and is easy to implement in Monte Carlo codes.

The stochastic mixing method is expected to become the default method in the next release of MONK, while the nearest temperature approach will be retained as a user option to allow direct comparisons between methods.

Acknowledgments

This work was supported by EDF Energy, and also by the McSAFE project of the European Union Horizon 2020 Research and Innovation Framework programme, grant No. 755097.

References

[1] S. D. Richards, C. M. J. Baker, P. Cowan, N. Davies, G. P. Dobson, MONK and MCBEND: Current Status and Recent Developments, Annals of Nuclear Energy 82 (2015) 63–73. doi:10.1016/j.anucene.2014.07.054.

[2] S. D. Richards, M. Shepherd, A. Bird, D. Long, C. Murphy, T. Fry, Recent Developments to MONK for Criticality Safety and Burnup Credit Applications, in: Proceedings of International Conference on Mathematics and Computational Methods Applied to Nuclear Science and Engineering, Jeju, South Korea, 2017.

[3] S. D. Richards, G. P. Dobson, D. Hanlon, R. J. Perry, F. Tantillo, T. C. Ware, MONK11A: Status and Plans for the MONK Monte Carlo Code for Criticality Safety and Reactor Physics Analyses, in: Proceedings of International Conference on Mathematics and Computational Methods Applied to Nuclear Science and Engineering, Portland, Oregon, USA, 2019. In press.

[4] R. J. Brissenden, A. R. Garlick, Biases in the Estimation of K_{eff} and its Error by Monte Carlo Methods, Annals of Nuclear Energy 13 (1986) 63–83. doi:10.1016/0306-4549(86)90095-2.

[5] WIMS: A Modular Scheme for Neutronics Calculations. User Guide for Version 10, ANSWERS Software Service, 2014.

[6] C. Dean, R. Perry, R. Neal, A. Kyrieleis, Validation of Run-Time Doppler Broadening in MONK with JEFF3.1, Journal of the Korean Physical Society 59 (2011) 1162–1165. doi:10.3938/jkps.59.1162.

[7] MONK: A Monte Carlo Program for Nuclear Criticality Safety and Reactor Physics Analyses. User Guide for Version 10B, ANSWERS Software Service, 2017.

[8] M. Herman, A. Trkov, ENDF-6 Formats Manual - Data Formats and Procedures for the Evaluated Nuclear Data Files ENDF/B-VI and ENDF/B-VII, National Nuclear Data Center, Brookhaven National Laboratory, 2009. doi:10.2172/981813, CSEWG Document ENDF-102, Report BNL-90365-2009 Rev. 1.

[9] K. Ivanov, M. Avramova, S. Kamerow, I. Kodeli, E. Sartori, E. Ivanov, O. Cabellos, Benchmarks for Uncertainty Analysis in Modelling (UAM) for the Design, Operation and Safety Analysis of LWRs. Volume I: Specification and Support Data for Neutronics Cases (Phase I), Technical Report NEA/NSC/DOC(2013)7, OECD Nuclear Energy Agency, 2013.